Determination of Morphologically Characteristic PCG Segments from Spectrogram Image*

Ana M. Gavrovska, *Student Member, IEEE,* Milorad P. Paskaš, *Student Member, IEEE* and Irini S. Reljin, *Senior Member, IEEE*

***Abstract* — The three-dimensional presentation of phonocardiac signal, simultaneously considering time, amplitude and frequency, allows the determination of morphological characteristic segments in phonocardiogram (PCG), both in short and long sequences. For this purpose, the STFT (Short-Time Fourier Transform) spectrogram images were used. By applying some methods known from image processing it is possible to recognize and extract basic heart sounds and murmurs from such time-frequency images. The method is tested over several characteristic test phonocardiac signals.**

***Keywords* — Morphological processing, murmur, phonocardiogram, spectrogram, STFT.**

I. Introduction

USING digital stethoscopes for acquiring digital records of heart sounds, phonocardiograms (PCG), provide a better insight into early diagnostics of heart diseases. Analysis of PCG signal in order to determine morphological characteristics may establish the possible existence of hemodynamic anomalies [1]. Determination of a potential cardiac problem from such quasiperiodic signals, based only on a few heartbeats, can be very useful for physicians to review and utilize these discoveries efficiently.

Time domain PCG analysis does not provide a clear insight into the frequency content of components, but is important [2] in order to get to know when a certain cardiac event has occurred, which heart sound has occurred, as well as the origin of murmurs, abnormal heart sounds like extra noise that blood makes as it flows through the heart [3],[4]. Unlike time domain, frequency domain provides an insight into the frequency content of PCG, but does not provide information about which frequencies are dominant in which moment, that is necessary to characterize appropriate events. Joint time-frequency analysis allows the simultaneous examination of both domains and as result we get a three-dimensional presentation of PCG. Simultaneous time, amplitude and frequency presentation represents an excellent way for precise determination of cardiac events and noise origin.

The purpose of this paper is to introduce morphological processing of PCG spectrogram image as a tool for distinguishing basic heart sounds and murmurs. This approach was applied to STFT (Short-Time Fourier Transform) images that are briefly discussed in section II. In section III we give a short overview of the basic concepts of morphological processing. The problem that we want to solve here is defined in section IV. Method of analysis is described in section V, where we conducted testing on five different characteristic signals with confirmed diagnosis. Section VI concludes the paper and it is mainly devoted to future research.

II. 3D Presentation using STFT

STFT resolves the time visibility problem of the nonstationary signal harmonic analysis. True joint time-frequency information is impossible to get, but spectral components can be seen within the time intervals. For a window function $w(t)$ in time domain, stationarity of the signal $x(t)$ is assumed within each segment, i.e. window, where the STFT of this signal is given by

$$STFT_x\{\omega,\tau\} \equiv X(\omega,\tau) = \int_{-\infty}^{\infty} x(t)w(t-\tau)e^{-j\omega t}\,dt\,. \quad (1)$$

If the window length is smaller, the time resolution is better but the frequency resolution is worse, and vice versa. In a discrete case, the STFT is calculated as:

$$STFT_x\{\omega,m\} \equiv X(\omega,m) = \sum_{n=-\infty}^{\infty} x(n)w(n-m)e^{-j\omega t}\,. \quad (2)$$

In JTFA (Joint Time-Frequency Analysis) we simultaneously use both time and frequency domain, while STFT is only one of the possibilities of such approach. As a result we get the spectrogram - an image of the spectral density $|X(\omega,m)|^2$, which is often used in applications for audio and speech signals [5],[6]. In this paper, STFT is chosen for JTFA, because it closely resembles the original appearance of signals observed through identical time-frequency localization windows.

***The "Ilija Stojanović" award for the best scientific paper presented at Telecommunications Forum TELFOR 2009.**

A. M. Gavrovska, PhD stipendiary of the Ministry of Science and Technological Development, Republic of Serbia, is with the Faculty of Electrical Engineering, University of Belgrade, Bulevar Kralja Aleksandra 73, 11120 Belgrade, Serbia; (phone: 381-11-3370143; e-mail: anaga777@gmail.com).

M. P. Paskaš is with the Innovation Center of the Faculty of Electrical Engineering, University of Belgrade, Bulevar Kralja Aleksandra 73, 11120 Belgrade, Serbia; (phone: 381-11-3370143; e-mail: milorad.paskas@gmail.com).

I. S. Reljin is with the Faculty of Electrical Engineering, University of Belgrade, Bulevar Kralja Aleksandra 73, 11120 Belgrade, Serbia; (e-mail: irinitms@gmail.com).

III. Introduction to Morphological Processing

The mathematical morphology methods have a significant role in image processing [7], where operations of dilation and erosion are fundamental. The dilation, denoted $A \oplus B$, that "thickens" objects in the binary image A controlled by structuring element B, is defined as:

$$A \oplus B = \left\{ z \left| \left(\hat{B} \right)_z \cap A \neq \varnothing \right. \right\}. \quad (3)$$

Unlike dilation, the operation of erosion, $A \ominus B$, that "thins" objects in the image, is defined as:

$$A \ominus B = \left\{ z \left| \left(B \right)_z \cap A^C \neq \varnothing \right. \right\}. \quad (4)$$

These two operations can be combined in various ways, where morphological opening and closing are one of the most common. Opening, denoted $A \circ B$, represents the erosion followed by dilation, i.e. $\left(A \ominus B \right) \oplus B$, while closing, denoted $A \bullet B$, calculates the inverse sequence of the basic operations as $\left(A \oplus B \right) \ominus B$.

IV. Problem of Cardiac Events Distinguishing

In order to visually separate characteristic cardiac events in PCG signal, STFT spectrograms are processed as images, because except time intervals in which these events occur, there is a need for their frequency and amplitude distinction also.

For the basic heart sounds (S1, S2, S3, S4), it is usually said that they are low-frequency, while the heart noises, murmurs, are of the high-frequency nature. However, such distinction is only partially correct. There is a large overlapping of bands of these two sets and that is the main problem in detecting cardiac anomalies [8], [9]. For this reason, morphological processing with the goal to separate characteristic parts of image is not an easy task.

V. Method of Analysis

A. Analyzed cases

As a test-bed, the first channel of PCG from reference dataset [10] is used. Since the frequency sampling was 44.1 kHz, we carried out the decimation with the factor 100. Such signals were preprocessed with the Hamming window of the length of 128 samples, with two samples less for overlapping, and so spectrograms are formed. Substantial differences in results weren't noticed even for shorter windows (lengths of 64, 32 and even 16 samples).

Signals with five diagnoses confirmed by physicians were under consideration: normal, aortic stenosis, mitral stenosis, mitral regurgitation, and aortic regurgitation PCG.

Two beats of normal PCG signal and appropriate spectrogram are shown in Fig. 1.(a)-(b). Heartbeat consists of time intervals that are determined with S1 and S2 and they are called: systole and diastole, where diastole has a longer interval than systole. Murmur in the case of aortic stenosis (Fig. 2.(a)-(b)) can be recognized by the place of occurrence, to be precise in a midsystolic part of the heartbeat. Its envelope has a characteristic shape, with an initial tendency to increase, and then to decrease. Mitral stenosis (Fig.3.(a)-(b)) has characteristic middiastolic murmur. It is characterized by the envelope that narrows in the middle of diastole.

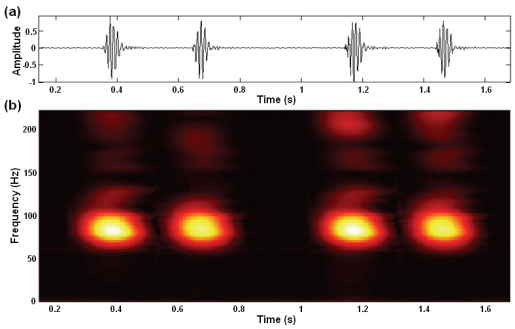

Fig. 1. (a) Normal PCG and (b) its spectrogram.

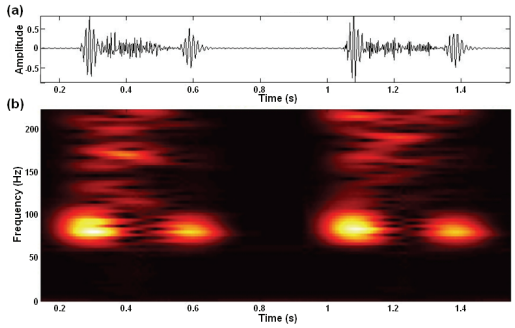

Fig. 2. (a) Aortic stenosis signal and (b) its spectrogram.

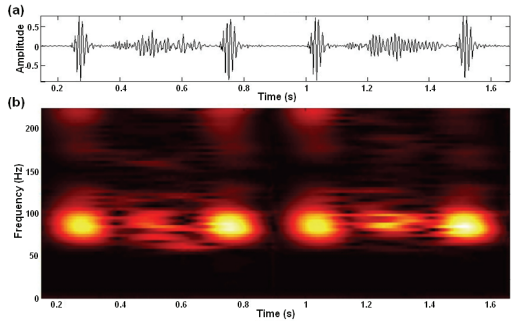

Fig. 3. (a) Mitral stenosis signal and (b) its spectrogram.

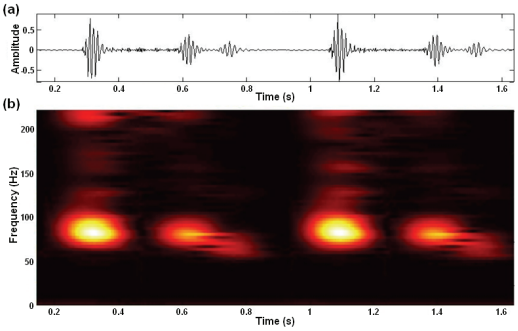

Fig. 4. (a) Mitral regurgitation signal and (b) its spectrogram.

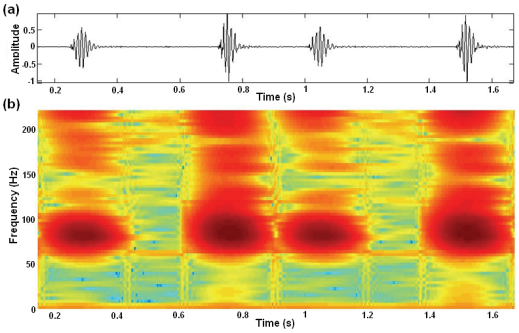

Fig. 5. (a) Aortic regurgitation signal and (b) its spectrogram.

Murmur may run continuously since the end of S1 to the start of S2 and then it is called holosystolic. In the case of mitral regurgitation, such murmur is shown in Fig. 4.(a)-(b). Early diastolic murmur that occurs in aortic regurgitation is the most difficult for physicians to detect (Fig. 5.(a)). The same case is with spectrogram, so in Fig. 5.(b) such colormap is set in order to make murmur more visible. This murmur has a tendency of decreasing since S2. In Fig.1-5. detection problem of heart anomalies that was explained in section IV is noticeable. In this paper, the primary goal was not murmur type recognition, but above all murmur identification and distinction from the basic heart sounds.

B. Morphological preprocessing of the spectrogram

As the first step toward making a distinction between relevant low-frequency and high-frequency components, original spectrogram is converted to a black and white (bw) mode in six ways.

The first three ways refer to individual work with columns of the matrix. In the first case, Fig. 6.(a), the threshold for each column was selected as its minimum increased by a standard deviation, in the second case, Fig. 6.(b), as its maximum reduced by a standard deviation, and in the third case, Fig. 6.(c), as its maximum reduced by 5% of the standard deviation.

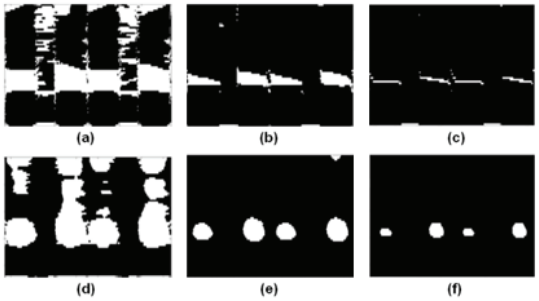

Fig. 6. (a)-(c) Thresholds for bw mode, when it comes to columns; (d)-(f) when it comes to whole matrix (case of aortic regurgitation).

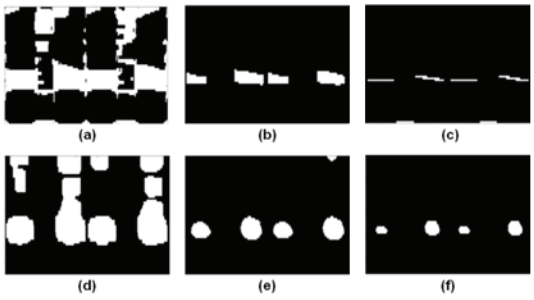

Fig. 7. (a)-(d) Morphologically preprocessed images Fig.6.(a)-(d); (e)-(f) as in Fig.6.(e)-(f) (case of aortic regurgitation).

For the next three ways in Fig.6. fixed thresholds are set for the whole matrices: the minimum of maximal values of columns increased by a minimal standard deviation, Fig. 6.(d), as well as increased by a maximal standard deviation, Fig. 6.(e), and the maximal value of the matrix reduced by 150% of the maximal standard deviation, Fig. 6.(f). Thus the six results are obtained setting two low, two medium and two high thresholds and contain all parts that might be relevant from the standpoint of energy for each column, as well as for the whole matrix. In Fig. 6. they can be seen for the case of aortic regurgitation.

Before establishing any correlation between these images, morphological preprocessing was performed in order to obtain better results. For Fig.6.(a), opening and closing was carried out with a 3x3 square as a structuring element, in order to shape the space that murmur occupies (see Fig. 7.(a)). For Fig. 6.(b) only opening is performed with a 4x4 square (see Fig. 7.(b)), and for Fig. 6.(c) opening with a horizontal line of the length ten is applied (Fig. 7.(c)), and for Fig. 6.(d) opening with 8x8 square (Fig. 7.(d)), so we get rid of the redundant details.

C. Simulation results

After the above mentioned preprocessing on the example of aortic regurgitation, as results that we wanted to obtain, we chose six of them, so they contain, respectively:

1. detected murmurs,
2. separated heart sounds,
3. precise enough heart sounds detection in time,
4. supporting artifacts from heart sounds (possibly with parts of murmurs relevant from the standpoint of energy),
5. extracted primary energy segments and
6. basic heart sounds presentation from the standpoint of energy.

Algorithm and the corresponding results will also be explained in the case of aortic regurgitation, which is a very difficult task for visual detection.

Separated heart sounds, Fig.8.(b), are obtained after morphological preprocessing (see Fig.7.(b)). After constructing a series of sums of each row of the matrix, from this series the longest subsequence of sums that are different from zeros is extracted, so that in Fig.8.(b) are shown only the rows from matrix that correspond to the chosen subsequence, thus the relevant low frequencies are chosen.

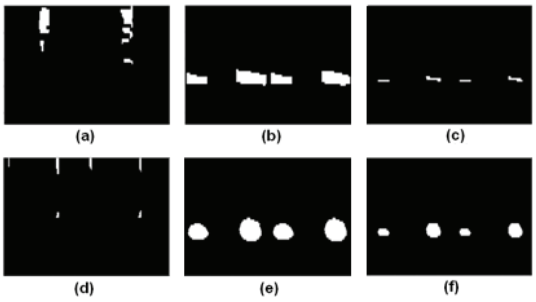

Fig. 8. (a)-(f) Results in the case of aortic regurgitation.

Detected murmur representation, Fig. 8.(a), can now be obtained by the rows and columns that correspond to separated heart sounds (Fig. 8.(b)) in the signal with appropriate diagnosis, and that we annul in the morphologically preprocessed image with a preset low threshold in dealing with columns (Fig. 7.(a)). After that, erosion is applied with a horizontal line of 20 pixels length as a structuring element.

Primary energy elements, Fig. 8.(e), and supporting artifacts, Fig. 8.(d), that are singled out, are obtained in the same way as in Fig. 8.(b) and Fig. 8.(a), respectively, using only Fig. 7.(e) and Fig. 7.(d) instead of Fig. 7.(b)

and Fig. 7.(a), respectively, and with no additional erosion applied.

Precise enough heart sounds detection in time, Fig. 8.(c), is obtained by the intersection of Fig. 7.(c) and Fig. 7.(f), while the representation of the basic heart sounds from the energy point of view, Fig. 8.(f), can be get by the intersection of Fig. 8.(b) and Fig. 8.(e).

As it can be seen in Fig. 8.(a)-(f), the algorithm in the case of aortic regurgitation gives excellent results.

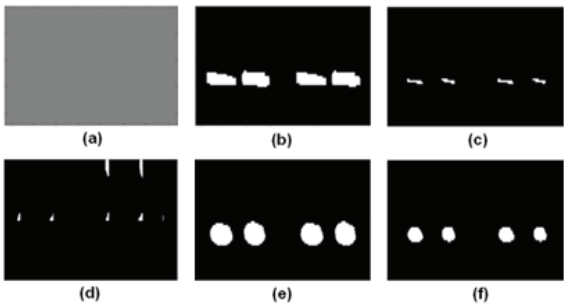

Fig. 9. (a)-(f) Results for normal signal.

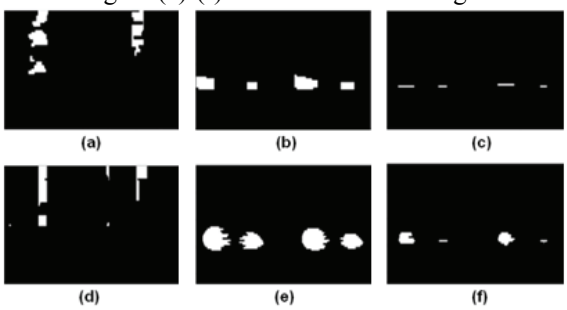

Fig. 10. (a)-(f) Results for aortic stenosis.

In Fig. 9.(a)-(f) the results are shown for a normal signal, obtained as previously described. By observing the specific normal signal in time domain, one cannot be assured of some potential murmur existence, but in a spectrogram, using the method described, no murmur was isolated, which is the expected result.

Results for aortic stenosis case can be seen in Fig. 10.(a)-(f). Murmurs and basic heart sounds are also well distinguished. It is not difficult to separate only artifacts of the basic heart sounds from murmurs using Fig. 10.(a) and Fig. 10.(d).

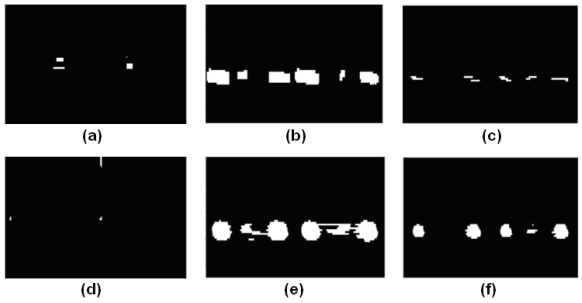

Fig. 11. (a)-(f) Results for mitral stenosis.

Mitral stenosis signal contained murmur that was mainly low-frequency, but it is obvious in Fig. 11.(a) that the existence of murmurs was detected.

In Fig. 12.(a) is the case where the second holosystolic murmur is not visible, but distinguishing heart sounds S1 and S2 from other low-frequency cardiac events can be seen clearly.

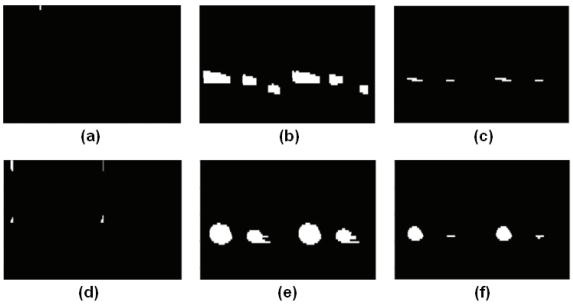

Fig. 12. (a)-(f) Results for mitral regurgitation.

Thus the proposed method gave excellent results in murmur detection and establishing sufficient accuracy for time durations of the basic heart sounds. It is necessary to accomplish even more subtle adjustments in this regard and establish different criteria for different heart sounds (e.g. for S1 and S2).

VI. Conclusion

Using a multiresolution analysis we can get at the same time better time and frequency resolution, especially in the case of nonlinear effects with fast and short changes. For that purpose it is necessary to make a comparison of available JTFA methods and corresponding spectrograms.

Further research will be addressed to improving analytical methods and exploring different ways to summarize these results in the field of quantitative phonocardiography by applying advanced methods for segmentation and recognition and artificial intelligence methods.

References

[1] M. I. Gabriel Khan, *On Call Cardiology*, Edition 3, Elsevier Health Sciences, 2006, pp. 30-50.

[2] A. Gavrovska, D. Jevtić, "Time-domain shape detection of murmurs in phonocardiograms," in *Proc. 53rd ETRAN Conference*, EK2.2-1-4, Vrnjačka Banja, June 15-18, 2009.

[3] F. Javed, P. A. Venkatachalam, A. Fadzil, "A signal processing module for the analysis of heart sounds and heart murmurs," *Journal of Physics*, *International MEMS Conference*, Series 34, 2006, pp. 1098-1105.

[4] A. K.Abbas, R. Bassam, *Phonocardiography Signal Processing*, Synthesis Lectures on Biomedical Engineering, University of Connecticut, Morgan&Claypool Publishers series, 2009.

[5] L. R. Rabiner, R. W. Scafner, *Digital Processing of Speech Signals*, Prentice Hall Signal Processing Series, 1978.

[6] A. V. Oppenhelm, R. W. Schafer and J. R. Buck, *Discrete-Time Signal Processing*, 2nd Edition, Prentice-Hall Signal Processing Series, 1999.

[7] R. C. Gonzalez, R. E. Woods and S. L. Eddins, *Digital Image Processing Using MatLab*, Prentice Hall, 2004, pp. 334-377.

[8] S. S. Tripathy, "System for diagnosing valvular heart disease using heart sounds," submitted thesis, Department of Computer Science&Engineering, Indian Institute of Technology, India, June, 2005.

[9] H. Jeharon, A. Seagar and N. Seagar, "Feature extraction from phonocardiogram for diagnosis based on expert system," in *Proc.27th Annu. International Conf. of the IEEE Engineering in Medicine and Biology Society* (EMBC '05), Shanghai, China, September 2005.

[10] Cardiothoracic Surgery of Savannah, Test Heart Sounds. Available: http://www.openheartsurgery.com/heart_sounds.html.